Adsorption energetics of Ag on MgO(100)

J. H. Larsen,* J. T. Ranney, D. E. Starr, J. E. Musgrove, and C. T. Campbell†
Department of Chemistry, University of Washington, 98195-1700 Seattle, Washington
(Received 27 July 2000; published 23 April 2001)

This paper reports experimental measurements of the interaction of Ag with MgO(100) thin films grown on Mo(100). Both the adsorption energy and the sticking probability of Ag gas are reported as functions of silver coverage at room temperature. The initial heat of Ag adsorption is ~176 kJ/mol, but increases rapidly with coverage, reaching the bulk silver heat of sublimation of 285 kJ/mol by ~8 ML. At the lowest coverages the sticking probability of silver is ~0.94 and approaches 1.0 with increasing coverage. Auger electron spectroscopy indicates that silver grows as three-dimensional (3D) islands from submonolayer coverages. From the integral heat of adsorption, the adhesion energy of silver to MgO is estimated to be 0.3 ± 0.3 J/m^2. The Ag-MgO(100) bond energy is estimated to be ~110 and ~15 kJ/mol within tiny 2D Ag clusters and large 3D Ag particles, respectively.

DOI: 10.1103/PhysRevB.63.195410 PACS number(s): 68.35.Md, 68.35.Np, 68.47.Jn, 81.15.Np

I. INTRODUCTION

Metal-oxide interfaces are used in a number of industrially important applications, e.g., in oxide-supported metal catalysts and microelectronics. In catalysis, the choice of metal and oxide support is critical in order to obtain a desired reactivity and selectivity. This is due in part to the inherent reactivity of the two components. Also the metal particle size and shape, which depend on the choice of oxide, can influence the catalytic activity dramatically. One of the parameters that determine the morphology of the particles is the strength of the interaction of the metal with the oxide substrate, which typically has a smaller surface energy than the metal. If there is a strong interaction energy, the metal tends to wet the substrate surface, and if the interaction energy is weak, the metal generally forms three-dimensional (3D) particles. The latter is often the case for equilibrium structures of late transition metals on typical support oxides[1–3] The description and understanding of the metal-oxide system is further complicated by the fact that morphological changes can be induced by the ambient gases; see, e.g., Refs. 4–6. In order to obtain a better understanding of these behaviors, there has been a number of investigations of model systems recently where the reactivity, particle size, and interactions of vapor-deposited metals with oxide substrates have been investigated experimentally[2–3,7–9] and theoretically.[10–15]

In this paper we will focus on the measurement of the adsorption energy of Ag on MgO(100). The general idea of a direct measurement of heats of adsorption of an adsorbate on a substrate is not new,[16] and a recent review of adsorption calorimetry methods and results can be found in Ref. 17. King and co-workers improved the experimental technique to allow for study on well-defined single-crystal surfaces,[18–21] giving important insight into both bonding strength and neighbor interactions of small molecules on single-crystal metal surfaces. In the Campbell group, adsorption on both metal and metal-oxide single-crystal surfaces were investigated, using a calorimeter setup similar to that of King and co-workers, with a different method of heat detection. Studies of Pb adsorption on Mo(100), oxidized Mo(100), and MgO(100)/Mo(100),[22–26] and Cu adsorption on oxidized Mo(100), MgO(100)/Mo(100), and disordered tungsten-oxide,[22,27,28] have been performed.

Oxide-supported Ag catalysts are extensively used for selective oxidation reactions, and there is therefore an interest in learning more about the interactions of Ag to oxide supports.[29] In the surface science community, there has been a considerable interest in the Ag-MgO model system,[30–42] and it was one of the first metal-oxide systems studied by surface science techniques.[43] The Ag-MgO(100) system has the appealing properties of having a small lattice mismatch of 3% (the lattice constant for Ag is 4.09 Å, and is 4.21 Å for MgO), and a cube-on-cube growth.[30–31,43] The influence of relaxations in the metal adlayers and in the top oxide layers on the growth is therefore expected to be negligible. This agrees well with theoretical findings for the Ag/MgO(100) system.[11]

The behavior of the measured heat of adsorption as a function of coverage depends on the growth mode. It was found by a number of groups that Ag on MgO(100) grows as 3D islands using various experimental techniques: Trampert *et al.* used TEM to study the Ag-MgO(100) system at somewhat elevated temperatures,[30] Robach, Renaud, and Barbier performed grazing incidence x-ray scattering experiments and analysis of crystal truncation rods at room temperature,[34,35] and Schaffner, Patthey, and Schneider used x-ray photoelectron spectroscopy (XPS) and electron-energy-loss spectroscopy to verify the 3D growth, also at room temperature.[33] It has, however, been argued by others that the growth is 2D at submonolayer coverages,[32,43,44] but, based on very definitive structural techniques and by reanalyzing previously reported data, it was recently suggested that the growth was 3D above 0.2 ML.[34–36] The islands were described as truncated pyramids with the (100) facet in contact with the substrate,[45] and a height-to-width ratio of ~0.4. The adsorption site was identified to be above oxygen in the MgO substrate,[34,35] which is in good agreement with theoretical studies of Ag adsorption on defect free MgO(100).[37,38,40,41] Recently, defects on MgO(100) were also investigated in cluster calculations, and it was found that a single metal atom [Rb, Pd, Ag (Ref. 42) and Cu, Ni, Ag, Pd (Ref. 41)] binds significantly more strongly there. This is in

good agreement with experimental evidence of defects acting as nucleation sites.[46]

Here we report experimental measurements of the adsorption energetics of Ag on a MgO(100) film grown on Mo(100) using single-crystal adsorption microcalorimetry. Sticking probabilities for Ag have also been measured. The adhesion energy, which is the binding energy per unit area at the interface between two condensed phases, has often been estimated from the energy required to separate a film from a substrate. Here it will be estimated based on the measured adsorption energies of Ag films on MgO(100). It contains important information on the strength of the metal-substrate interaction, and is often difficult to determine experimentally.[1–2,10] Many adhesion energies have been found by measuring the contact angle of liquid metal drops on metal oxides and then applying the Young-Dupré relation.[47–49] More recently, adhesion energies were reported for solid metal particles on ordered oxide surfaces from transmission electron microscopy measurements of the contact angle, e.g., for Ag particles on MgO(100) substrates,[30] and from scanning tunneling microscopy measurements of the height-to-width ratio for Pd particles on Al_2O_3 thin films.[50] Theoretical calculations of the adhesion energy of metal to oxides were also reported (see Ref. 10, and references therein), but it is not yet known how accurate the results are, partially because of a lack of reliable experimental data with which to compare.

II. EXPERIMENT

The ultrahigh-vacuum chamber used in this study has a base pressure below 1×10^{-10} mbar and is equipped with Auger electron spectroscopy (AES), low-energy electron diffraction (LEED), a quadrupole mass spectrometer (QMS), and a unique setup for measuring heats of adsorption of metals on thin single-crystal samples (~1 μm thick). From a chopped effusive vapor source, metal atoms can be deposited onto the single crystal surface in $\sim$100-ms pulses. See Refs. 22–24 and 28 for more details on the experimental setup and procedures.

For the heat detection, a flexible ribbon of pyroelectric β-polyvinylidene fluoride (PVDF) is used, with its front and back faces coated with 20–60 nm of NiAl for electrical contacts. The ribbon forms an arc, which is pressed gently up against the backside of the thin single-crystal sample for detection of adsorption heats. The voltage response of the PVDF ribbon to a heat pulse arising from an adsorbing gas pulse is converted into energy by calibrating the response to pulses of known energy from a He-Ne laser. The manufacturer-specified long-term intensity stability of the He-Ne laser used here is $\pm1.5\%$, and it has usually given this.[22–24] However, during the experiments reported here, it had intensity fluctuations $\sim$20-fold larger (see below), possibly due to turning on a fan nearby (discovered later to create problems). For this reason, the absolute calibrations for three runs were averaged here, and further adjusted by 4% to agree with the expected high-coverage result, as described in more detail below.

The measured heat signal contains additional contributions from the radiation of the effusive source and from the loss of kinetic energy of the impinging metal atoms to the substrate. The radiation contribution, determined when blocking the metal atoms with a BaF_2 window, accounts for $\sim$30% of the total signal in the case of Ag adsorption on MgO(100). Taking these additional contributions into account, with the addition of the pressure-volume work term (see Ref. 24 for more details on this procedure), recasts the measured energies into standard enthalpies of adsorption with both reactants and products at 300 K. These are the values actually reported below. This corrected heat of adsorption measured at high coverage, where the atoms are adding to bulklike sites, is thus directly comparable to the standard heat of sublimation of the metal. In order to obtain the energy of adsorption on a ''per mole adsorbed metal'' basis, it is divided by the amount of adsorbed Ag in each metal atom pulse, obtained by correcting the measured Ag flux (using a calibrated quartz crystal microbalance) with the experimentally determined sticking probability. The absolute sticking probability is found as a function of coverage by measuring the intensity of the reflected (nonsticking) Ag atoms in the QMS ($m/e=108$), and normalizing this to the time-integrated signal from total reflection off a hot Ta foil. This setup also enables the study of lifetimes of metal atoms on surfaces as a function of temperature.[25–26]

The cleanliness of the 1-μm-thick Mo(100) substrate is obtained by repeated heatings to high temperature and verified with AES. The MgO(100) film on Mo(100) is prepared by dosing high purity (99.9+%) Mg in an oxygen atmosphere with subsequent annealing to $\sim$750 K, as described by Wu and co-workers,[51,52] and previously used for microcalorimetric studies of Cu and Pb on MgO(100).[25–27] The MgO(100) film is $\sim$4 nm thick as estimated from AES analysis, and the (1×1) square symmetry pattern is observed with LEED of similar quality as in Refs. 51 and 52. No carbon or metallic Mg is observed by AES for the MgO films. The MgO(100) substrate is kept at room temperature (300 K) for all adsorption experiments, and heating the system after the adsorption experiment removes the Ag and leaves the MgO(100) thin film intact.

III. RESULTS

A. Adsorption energy and sticking probability

The heat of adsorption of Ag on MgO(100)/Mo(100) is shown in Fig. 1 as a function of the adsorbed Ag coverage in monolayers where 1 ML is defined as the packing density of a Ag(100) plane in bulk Ag, 1.2×10^{19} atoms/m^2. The curve is an average of three adsorption calorimetry experiments, all with pulses containing $\sim$0.03 ML of Ag per pulse (corresponding to a flux of $\sim$0.6 Å/s during each pulse, which lasts for 100 ms and repeats every 2.00 s). Since the fluxes were not exactly the same in these experiments, the signals for individual pulses were also averaged over a fixed coverage range, each 0.05 ML. The adsorption energy at the lowest coverage is $\sim$176 kJ/mol, and it increases up to a plateau at 285 kJ/mol for coverages above 8 ML. Some minor corrections have been made to the measured heats, as discussed above, to convert to standard heats (enthalpies) of

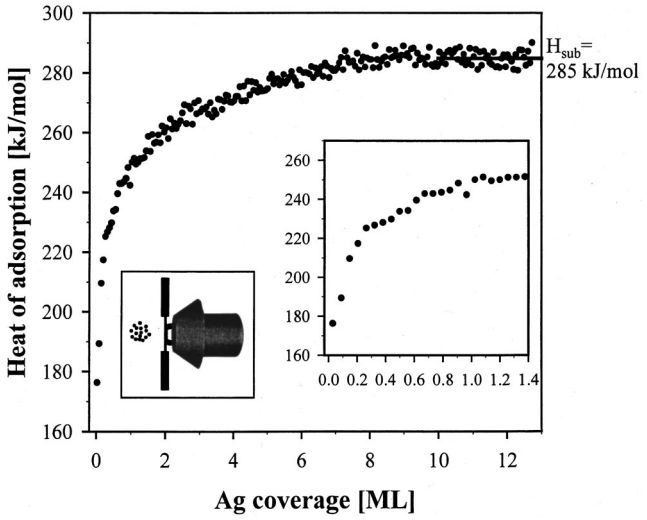

FIG. 1. The measured heat of adsorption of Ag on MgO(100) at room temperature as a function of the amount of Ag adsorbed. The heat of adsorption for the first 1.4 ML is shown in one inset, and an illustration of an impinging metal pulse onto the oxide surface with the heat sensitive ribbon in contact with the backside of the sample in another inset. [The flux is ~0.03 ML/pulse, corresponding to 3.6×10^{18} atoms/(s m^2) during 100-ms square-wave pulses with a repeat period of 2.00 s. The signal is averaged over 0.05-ML coverage increments.]

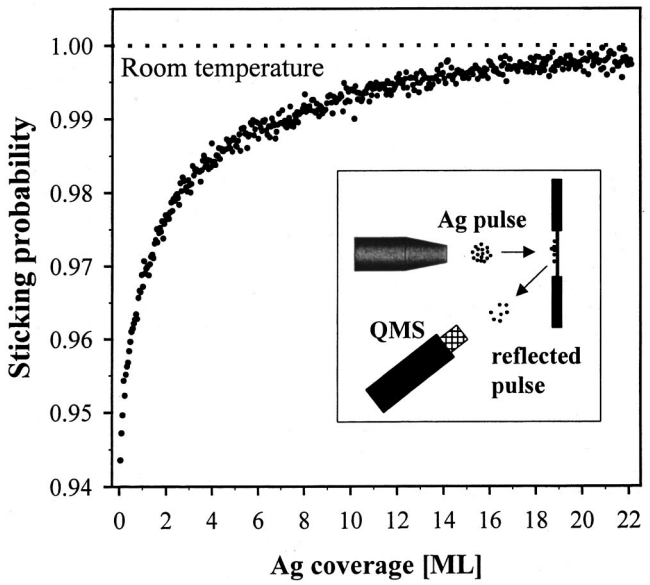

FIG. 2. The absolute sticking probability of Ag on the MgO(100) thin film is shown as a function of the adsorbed Ag coverage. The curve is an average of two experimental data sets. The sticking probability was found by measuring the QMS signal ($m/e=108$) of the reflected (nonsticking) Ag atoms. The experimental setup is illustrated in the inset. The pulse flux and repetition rate are the same as in Fig. 1.

adsorption at 300 K, and thus enable a direct comparison to the bulk enthalpy of sublimation. Due to temporary problems with laser instability during these experiments (see Sec. II), our absolute heat calibrations here were not as accurate as usual. The error in the calibration factor in individual runs was estimated by comparing the heat of adsorption obtained at 12 ML to the heat of sublimation of bulk Ag (285 kJ/mol),[53] which we assumed is the true value at 12 ML. The resulting systematic errors in absolute calibration were −23%, −20%, and +32% (compared to ~2% usually obtained[24]). This calibration error reduced to −4% upon averaging the three runs. Because of this residual −4% error, we scaled the averaged heats by 1.04 in order to force the adsorption energy at 12 ML to equal silver's heat of sublimation. When individually normalized, the three curves all showed very similar coverage dependences of the heats. (At any given coverage above 0.1 ML, their average deviation magnitude from the curve shown was <3%, and it averaged only 0.9% over the full coverage range. Their average deviation magnitude from the average curve shown was larger (~6%) for the pulses in the first 0.1 ML, possibly due to differences in surface defect densities of the starting surfaces, and the initial population of defect sites.) As can be seen, the point-to-point precision of the averaged curve at high coverage (where the heat is constant enough to estimate the scatter) is excellent (standard deviation <2 kJ/mol, or ~0.7%).

In Fig. 1, the adsorbed amount of Ag was obtained by scaling the measured incident amount of metal with the corresponding sticking probability. This sticking probability is reported in Fig. 2 as a function of the adsorbed Ag coverage. In the inset, the setup is shown schematically. The data are an average of two measurements. Initially, the sticking probability of Ag on clean MgO(100) is ~0.94, and it increases with increasing silver coverage, reaching 1.00 above ~20 ML.

B. Growth of Ag on MgO(100)

The growth of Ag on MgO(100) was investigated with AES. In Fig. 3, the normalized peak-to-peak signal of the 356-eV Ag AES peak is shown as a function of the adsorbed Ag coverage, using a continuous Ag beam of the same time-averaged flux as (but much lower peak flux than) the pulsed-beam experiments of Figs. 1 and 2. (In Fig. 3, the beam was interrupted during each AES measurement.) Above 30 ML of adsorbed Ag, the oxygen signal at 510 eV was attenuated below our detection limit, and it was therefore reasonable to use the average of the data points above this high coverage as representative of a saturation signal for bulk Ag. The detection limit was estimated from the signal-to-noise level to be ~10% ML. The details of the growth of the first 6 ML are shown in the inset. The dashed line in Fig. 3 shows the expected AES intensity for a layer-by-layer growth model for comparison. A mean free path for the Ag Auger electrons of 7.1 Å was used.[54] Note that by 0.5 ML of Ag adsorbed, the AES data deviates from the layer-by-layer model and fall significantly below this model, suggesting 3D island growth.

The literature provides experimental evidence for the growth of Ag on MgO(100) being 3D islands,[34–36] and we therefore also compare our data to a growth model assuming hemispherical shaped particles (solid line).[55] The single fitting parameter in this model is the island density, and the model is only valid before island coalescence begins. The

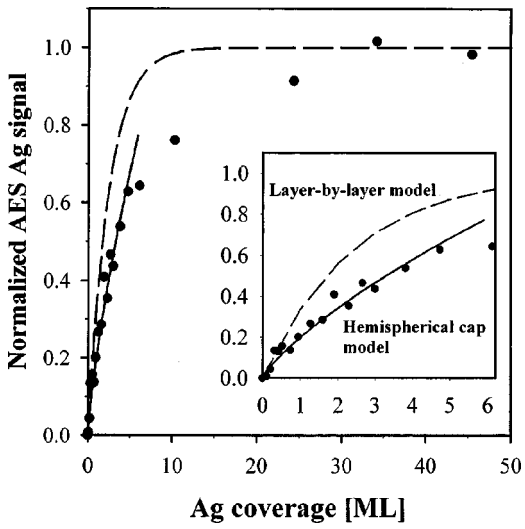

FIG. 3. The normalized intensity of the 356-eV Ag Auger line (circles) is shown as a function of the adsorbed Ag amount. The dashed line describes a simple layer-by-layer growth behavior, and the solid line is the best fit of a model based on a constant number of Ag particles shaped as hemispherical caps, described in more detail in the text. The inset shows coverages below 6 ML in more detail. The flux is ~0.01 ML/s (continuous beam).

best fit to the data below 6 ML gives a hemispherical island density of 2.5×10^{16} m^{-2}, and the mean radius of the particles increases up to 32 Å at 6 ML. It is clear in the inset that the hemispherical model is far superior to the layer-by-layer model above 0.5 ML. At coverages below ~0.3 ML, however, the layer-by-layer growth model describes the data slightly better, suggesting the growth of mainly 2D islands below ~0.3 ML. The simple hemispherical model fit below 6 ML does not allow for a variation in the island density with coverage. One could argue that it would be necessary to include such a variation if a description of the growth in the entire coverage interval is required. Such an analysis was performed by Renaud and co-workers for the Ag/MgO(100) system,[34–36] and, indeed, a decrease in island density from $\sim3\times10^{16}$ m^{-2} at the lowest coverages, to below 0.5×10^{16} m^{-2} above 12 ML, was found. It is, however, beyond the scope of this paper to go into such a detailed growth analysis of our data. In the following it will become important to know the fraction of the surface covered by Ag. Assuming that the Ag islands at ~8 ML are thick enough over most of their area to produce bulklike Ag AES signals, then the measured signal relative to bulk Ag can be used to estimate the Ag-covered fraction of the surface. Using this assumption, approximately 70–80 % of the surface is covered with Ag islands at 8 ML. Above ~30 ML we do not detect any oxygen signal, suggesting that the MgO surface is >90% covered with Ag. The authors of Ref. 34 found that their bulk MgO(100) surface is ~80–90 % covered with Ag at a coverage of 8–14 ML.[34]

IV. DISCUSSION

The absolute value of the initial sticking coefficient for Ag on MgO(100) films at room temperature, as shown in Fig. 2, is ~0.94. In a room-temperature experiment[33] of Ag sticking on a MgO(100) thin film, a lower sticking probability (~0.6) was estimated from XPS. The sticking coefficient should increase with the number of Ag islands per unit area present on the surface. The larger the island density, the shorter the time that a transiently adsorbed, isolated Ag adatom must spend diffusing in between islands before attaching to an island, and therefore the lower the probability of it desorbing rather than permanently sticking. The density of defects often influences the saturation density of metal islands in vapor deposition.[2,56–58] The MgO thin films used in the study in Ref. 33, and in the present study, were prepared the same way, so we can expect similar defect densities. The incident metal fluxes in the two studies are, however, very different. The authors of Ref. 33 used a flux of ~0.5 Å/min, while we employed an 80-fold larger flux of ~40 Å/min (during the pulse) in Figs. 1 and 2. It is well known that the saturation density of islands also depends on the incident metal flux (the island density is proportional to the flux to the power of 1/3 under many conditions[2,56–58]). Using this relationship, the Ag island density in our experiment will be approximately four times larger than in the study by of Ref. 35, and this could very well be the origin of our higher sticking probability.

The measured heat of adsorption in Fig. 1 is initially 176 kJ/mol. It rises steeply up to a coverage of ~0.2 ML, as seen in the inset, and then increases more slowly finally reaching the bulk Ag-Ag interaction energy, the heat of sublimation of 285 kJ/mol[53] around 8 ML. The initial adsorption sites are probably steps and/or defects, which are well known to exhibit stronger bonding to metal atoms and thus act as nucleation sites.[2,41–42,59] For example, it has been observed for Pd on MgO(100) with transmission electron microscopy[3] and with atomic force microscopy[46] that the metal islands preferentially nucleate along defects and steps, illustrating the preferred and stronger bonding. The initial population of defects followed by mainly terrace sites, by itself, would cause the adsorption energy to decrease with coverage. This effect is overpowered by the increase in the average Ag-Ag coordination number with island size, giving rise to the steep increase in heat with coverage.

To estimate the strength of the initial Ag/MgO interaction from the calorimetry results, one can employ a simple pairwise bond additivity approximation. While this model is inaccurate in details, it has been used with great success in understanding qualitative aspects of many chemical reactions, and so we use it here as a first-order estimation. We first assume that the Ag islands formed on the initial 0.03-ML pulse are predominately 2D, as suggested by AES. We further assume that the Ag island density at 0.03 ML is the same as seen for 3D particles at higher coverages ($\sim2.5\times10^{16}$ m^{-2}), which gives an average island size of 14 atoms. (After a saturation density is reached at very low coverage, island densities often stay relatively constant until the islands start to coalesce at very high coverage.[2,58,59]) Assuming square close packing in a compact 2D island, the average island will then have ~20 Ag-Ag nearest-neighbor bonds. If each of these bonds has the same strength as in bulk Ag, i.e., one-sixth of the silver heat of sublimation

$(1/6\times 285\ \text{kJ/mol}=47.5\ \text{kJ/mol})$, then the average atom deposited in the first pulse is stabilized by $(20/14)\times 47.5\ \text{kJ/mol}=68\ \text{kJ/mol}$ in Ag-Ag bonds alone. The initial adsorption energy is ~176 kJ/mol so the excess amount of stability is due to the Ag-MgO bond to the substrate. Subtracting the Ag-Ag interactions, one arrives at a value of ~110 kJ/mol for the average bond energy between an Ag atom in this 14-atom 2D island and the MgO(100) substrate. Using the atomic density of the Ag(100) facet, this corresponds to an adhesion energy between 2D Ag(100) islands and MgO(100) of ~2.2 J/m^2. Since the Ag-Ag bonds in small particles are expected to be stronger than the corresponding bulk bonds,[67] and since defects probably strengthen the Ag-MgO bonds, the estimates found above for the bond energy and adhesion energy must be considered upper limits.

If one instead assumes that the 14-atom clusters formed in the first pulse make a pyramidal 3D island with nine Ag atoms in the first layer, four in the second and one on top (thus forming 36 Ag-Ag nearest-neighbor bonds), then Ag-Ag pairwise bonding contributes $(36/14)\times 47.5\ \text{kJ/mol}=122\ \text{kJ/mol}$ to the initial adsorption energy, leaving only 54 kJ/mol for the average Ag-MgO pairwise bond energy. However, since only nine of the Ag atoms have MgO nearest neighbors in this geometry, their Ag-MgO bond energies are $(14/9)\times 54\ \text{kJ/mol}=84\ \text{kJ/mol}$. This corresponds to an adhesion energy of 1.7 J/m^2 for these tiny 3D clusters to the MgO(100) surface. Since the pulse flux in Fig. 1 was actually higher than in the AES measurements used to estimate island density, the island density is probably higher and the island size smaller than in the above calculations. Correcting for this would lead to even larger estimates of the Ag-MgO bond energy and adhesion energy.

Additional insight into the interaction strength of the Ag to the MgO substrate can also be gained by determining the adhesion energy of 3D Ag islands. Integrating the calorimetric heat of adsorption, q_{cal}, reported in Fig. 1 from zero to multilayer coverages provides a route for estimating this adhesion energy. The principle is based on a simple thermodynamic cycle derived elsewhere.[2,22] The enthalpy change of two different pathways is considered: from an initial state of n moles of gaseous metal atoms and a clean oxide surface, to a final state of an oxide-supported multilayer metal film with interfacial area A and surface energy γ. The evaluation results in the following expression for the adhesion energy of the metal-to-oxide interface:

$$E_{\text{adhesion}}=(1+f)\,\gamma-\left(n\times\Delta H_{\text{sub}}-\sum_{n} q_{\text{cal}}\right)\Big/ A. \quad (1)$$

Here f is the roughness factor of the resulting metal-vacuum interface, and ΔH_{sub} is the heat of sublimation of bulk Ag (285 kJ/mol).[53] The value of the surface energy γ of solid bulk Ag was taken to be 1.22 J/m^2,[60] which is in good agreement with theoretical values for the low-index facets [1.30 J/m^2,[61] 1.21–1.26 J/m^2,[62] and 1.17–1.24 J/m^2 (Ref. 63)]. (For metals, the surface energy and surface free energy are almost the same at 300 K, since vibrational entropy is small.) The first term in Eq. (1) relies on information on the growth morphology via the roughness factor f, and the second term is determined by integrating our measured heats of adsorption from Fig. 1. One should apply Eq. (1) to a large multilayer Ag coverage for which the morphology is best known, which is at ~6–8 ML where large particles of Ag (as opposed to a continuous Ag film) are grown. In such cases, the area A is the total surface area of the Ag particle/MgO(100) interfaces, and f refers to the ratio of the Ag/vacuum area to the Ag/MgO area. Inspection of Fig. 1 furthermore gives that the integration has to be performed up to at least ~8 ML, where the adsorption energy appears to first reach the bulk sublimation energy plateau. Since errors in absolute calibration of the calorimeter amplify in their contribution to E_{adhesion} when larger coverages are used than at the apparent achievement of the bulk cohesive energy, we integrate Eq. (1) up to 8 ML only.

The authors of Ref. 34 modeled x-ray scattering data of Ag/MgO(100) with Ag particles shaped as truncated pyramids stacked as (100) layers, and found a coverage-independent height-to-width ratio, corresponding to a roughness factor of 1.6. Using this value of f and their result that the Ag particles cover 80 to 90 % of the surface at 8 ML, we calculate an adhesion energy of 0–0.04 J/m^2 from Eq. (1). (The range actually extends to $-0.3\ \text{J/m}^2$, but we omit the negative values since they are physically unreasonable.) Assuming instead a hemispherical cap shape ($f=2.0$) which fit our Auger data at 1 to 6 ML, and our AES result that the Ag particles cover ~70–80 % of the surface at 8 ML, we find an adhesion energy of 0–0.2 J/m^2. (Again, the range actually extends to $-0.2\ \text{J/m}^2$.) It should be emphasized that these numbers are very sensitive to the parameters used, e.g., by using 1.30 J/m^2 instead of 1.22 J/m^2 for the surface energy of bulk Ag, the adhesion energies become ~0.2 J/m^2 larger. Also, the expected error bars in the heat calibration lead to errors in E_{adhesion} of $\pm 0.3\ \text{J/m}^2$. Nevertheless, we can conclude that the adhesion energy of Ag to MgO is small, with an absolute value in the range of 0–0.6 J/m^2. For comparison, we found a value of $2.2\pm 0.3\ \text{J/m}^2$ for Cu/MgO(100).[27] (Note that the absolute error bars are the same, but the relative error is much less for Cu.) The observed adhesion energy of Ag($0.3\pm 0.3\ \text{J/m}^2$) implies an equilibrium contact angle θ_C of $\sim 150°\pm 30°$ according to the Young-Dupré equation:[1] $\cos\theta_C=[(E_{\text{adhesion}}\gamma)-1]$.

Experimental and theoretical adhesion energies for Ag on MgO(100) were reported previously,[30,31,38,64] but with no general agreement in the value. Trampert *et al.*[30] found 0.45 J/m^2 on cleaved MgO surfaces by measuring the contact angle with transmission electron microscopy. Theoretical values are in general higher: Schönberger, Andersen, and Methfessel reported a value of 1.6 J/m^2 based on density-functional theory,[31] Smith, Hong, and Srolovitz found values around 1.0 J/m^2,[64] and Zhukovskii *et al.* reported 0.83 J/m^2 using Hartree-Fock calculations.[38] Finnes argued in a recent review on metal-ceramic interfaces that theoretically determined adhesion energies are likely to exceed the experimental estimates due to misfit dislocations, which reduce the measured adhesion.[10] The adhesion of molten Ag on other oxide surfaces has also been found from contact angle measurements, e.g., for Ag/SiO_2 (Ref. 65) and $\text{Ag/Al}_2\text{O}_3$.[48] In both cases, the adhesion energy was found to be 0.2–0.3

J/m^2. Didier and Jupille previously argued that the adhesion energy changes with the oxide band gap,[66] and a comparison of the adhesion of the same metal to MgO, SiO_2, and Al_2O_3 therefore seems relevant since their band gaps are similar.[1] Our estimated adhesion energy for Ag on MgO(100) is thus in good agreement with the adhesion energies of Ag on SiO_2 and Al_2O_3.[65,48]

The observed adhesion energy of 0.3 ± 0.3 J/m^2 for large 3D particles corresponds to a bond energy of Ag to MgO(100) of 15 ± 15 kJ/mol [assuming an Ag(100) packing density]. This is ~7-fold weaker than determined between 2D Ag platelets and MgO(100) (~110 kJ/mol, from above). The atoms in 2D Ag islands bond much more strongly to the oxide below than do those in 3D islands. Also, oxide surface defects are more commonly sampled at the interface in the 2D island measurements (which covered only 3% of the surface). In the case of Cu/MgO(100), the bond energy was estimated for 2D islands at a much higher coverage (~30% of a ML) such that defects should not play such a strong role. Even there, the Cu atoms in 2D Cu islands bond to MgO twice as strongly as do Cu atoms in thick, 3D islands, within the bond additivity model.

This qualitative difference between metal-oxide interfacial bonding at 2D versus 3D islands can be understood within a bond-energy–bond-order conservation picture: Since the metal atoms in 2D islands are coordinately unsaturated, they do not have to use ''bonding facility'' to interact with metal atoms in the layer above, and they thus bond with greater energy to the MgO below. This, of course, is a failure of bond additivity, which is common in late transition metals, and gives rise, for example, to stronger metal-metal pairwise interaction energies in particles of a few atoms than in bulk metal.[67] Note that in both 2D and 3D islands, Ag bonds more weakly to MgO(100) than does Cu (see Ref. 27), in good agreement with theoretical results by Matveev *et al.*[40]

Figure 4 summarizes our results within a bond additivity model. Packing within all Ag layers is assumed here to be (100)-like parallel to the surface, with all Ag-Ag bonds parallel to the surface having their bulklike strength (the bond energy is 47.5 kJ/mol). The top schematically shows a small (~14 atom) 2D Ag island as produced in the first pulse of Fig. 1. The average heat of adsorption, q_{cal}, is shown, as well as the average bond energy of these Ag atoms to the MgO below. The bottom shows a large 3D Ag island as produced at ~8-ML coverage. The Ag atoms at its bottom surface have a much weaker bonding to the MgO below (~15 kJ/mol). Ag atoms within the bulk bind to the Ag(100) layer below with four Ag-Ag bonds, giving a total bond energy of $4\times47.5=190$ kJ/mol. The undercoordinated Ag atoms in the topmost atomic plane of Ag(100) must bind to the layer below more strongly than in the bulk. That is, if pairwise bond additivity actually held, the Ag(100) surface energy would be equal to two Ag-Ag bonds per atom, 2×47.5 kJ/mol$=95$ kJ/mol$=1.89$ J/m^2, not the true value of 1.22 J/m^2. Since we assume in this simplified bond additivity model that the in-plane bonds remain the same in the topmost Ag(100) layer, the Ag bond strength to the layer below must be increased by $1.89-1.22$ J/m$^2=0.67$ J/m^2, or 34 kJ/mol, to compensate for this difference. Since there are four bonds per atom to the layer below, this only corresponds to an increased bonding of 8.5 kJ/mol per Ag-Ag bond. While the above assumes that all Ag-Ag bonds parallel to the surface have their bulk strength, actually these are expected to be slightly stronger within the topmost (bottommost) atomic planes, assuming bond energy-bond-order conservation, since these Ag atoms have no (weaker) bonding partners in the layer above (below).

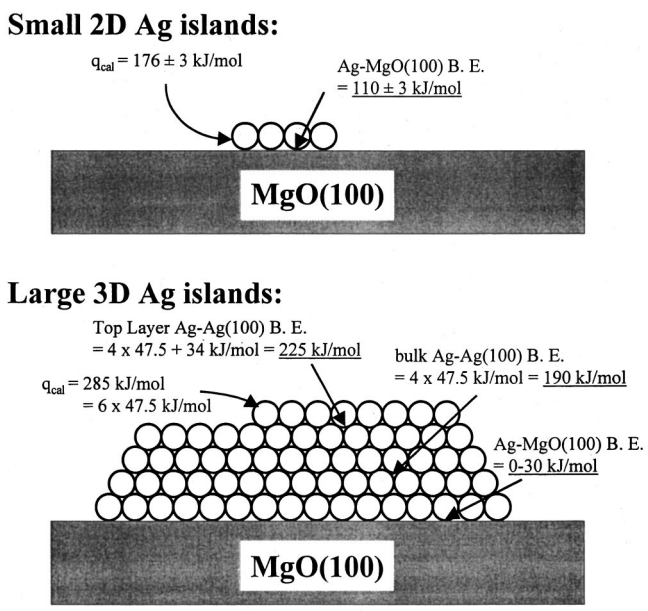

FIG. 4. Heats of adsorption (q_{cal}) and bond energies for Ag atoms to MgO(100) and Ag(100) planes for tiny 2D clusters and large 3D Ag particles. Here B. E. refers to the total bond energy between one Ag atom and all atoms in the layer below it to which it bonds. They are calculated assuming Ag(100)-like packing and pairwise bond additivity, with bulklike in-plane Ag-Ag pairwise bond energies ($=\Delta H_{sub}/6=47.5$ kJ/mol). For the small 2D islands, the bond energy of a Ag atom to the MgO substrate was found by subtracting the in-plane Ag-Ag bond energy contribution from the measured initial heat of adsorption of 176 kJ/mol, resulting in 110 kJ/mol. In the case of large 3D islands, a much smaller bond energy of 15 ± 15 kJ/mol was found from the measured adhesion energy (0.3 ± 0.3 J/m^2). For details, see the text.

We now have measured heats of adsorption and sticking probabilities of Cu,[27] Pb,[25] and Ag (present study) on similarly prepared MgO(100) surfaces. Pb has the smallest initial adsorption energy of ~100 kJ/mol; then follows Ag, with ~176 kJ/mol and finally Cu at ~240 kJ/mol. In all three cases, we have measured an energy difference of ~100 kJ/mol between the initial adsorption energy and the heat of sublimation (Pb 195 kJ/mol; Ag: 285 kJ/mol; Cu: 337 kJ/mol).[53] The order of the adsorption energies follows the order of the adsorption probabilities: The initial sticking coefficient for Pb is ~0.7, and it increases only slowly. For Ag the initial sticking is only slightly below unity (~0.94), and Cu adsorbs with a close to unity probability even during the very first Cu metal pulses. A more detailed comparison of these measured quantities is given in Refs. 25 and 26 along with a discussion of the magnitude and origin of the adhe-

sion energies for Ag, Cu, and Pb to MgO(100), and a comparison to various proposed models for the adhesion energy behavior.

V. CONCLUSIONS

In this paper we have investigated the growth mode, adsorption energy, and sticking probability of Ag on MgO(100)/Mo(100). From AES, the growth mode is found to be as 3D islands above 0.5 ML, in agreement with recent experimental investigations. Furthermore, it was found that the Ag atoms interact weakly with MgO(100), with an initial adsorption energy of only ~176 kJ/mol and a sticking probability of 0.94. The adsorption energy increases with coverage, and reaches the bulk heat of sublimation of 285 kJ/mol above 8 ML. The weak Ag-MgO interaction is further supported by the Ag/MgO(100) adhesion energy of $0.3 \pm 0.3\ J/m^2$ estimated from the measured heat of adsorption, integrated from zero to multilayer coverage. The Ag-MgO(100) bond energy is estimated to be 110 kJ/mol for Ag atoms in small 2D clusters (probably nucleated at defects), and 15 kJ/mol for large 3D Ag particles.

ACKNOWLEDGMENTS

The National Science Foundation and the University of Washington Center for Nanotechnology are acknowledged for financial support, and Jacques Chevallier at University of Aarhus, Denmark, is very sincerely thanked for supplying the high-quality single crystals used in this study.

*Present address: Interdisciplinary Research Center for Catalysis (ICAT), Department of Physics, Technical University of Denmark, DK-2800 Kgs. Lyngby, Denmark.

†Author to whom correspondence should be addressed.

[1] C. Noguera, *Physics and Chemistry at Oxide Surfaces* (Cambridge University Press, Cambridge, 1996).
[2] C. T. Campbell, Surf. Sci. Rep. **27**, 1 (1997).
[3] C. R. Henry, Surf. Sci. Rep. **31**, 231 (1998).
[4] B. S. Clausen, J. Schiøtz, L. Gråbæk, C. V. Ovesen, K. W. Jacobsen, and J. K. Nørskov, Top. Catal. **1**, 367 (1994).
[5] C. V. Ovesen, B. S. Clausen, J. Schiøtz, P. Stoltze, H. Topsøe, and J. K. Nørskov, J. Catal. **168**, 133 (1997).
[6] H. Graoui, S. Giorgio, and C. R. Henry, Surf. Sci. **417**, 350 (1998).
[7] P. L. J. Gunter, J. W. Niemantsverdriet, F. H. Ribeiro, and G. Somorjai, Catal. Rev. Sci. Eng. **39**, 77 (1997).
[8] D. W. Goodman and D. R. Rainer, J. Mol. Catal. **131**, 259 (1998).
[9] H. J. Freund, Faraday Discuss. **114**, 1 (1999).
[10] M. W. Finnes, J. Phys.: Condens. Matter **8**, 5811 (1996).
[11] J. Goniakowski, Phys. Rev. B **57**, 1935 (1999).
[12] C. Verdozzi, D. R. Jennison, P. A. Schultz, and M. P. Sears, Phys. Rev. Lett. **82**, 799 (1999).
[13] D. R. Jennison and A. Bogicevic, Faraday Discuss. **114**, 45 (1999).
[14] A. M. Ferrari, C. Y. Xiao, K. M. Neyman, G. Pacchioni, and N. Rösch, Phys. Chem. Chem. Phys. **1**, 4655 (1999).
[15] K. M. Neyman, N. Rösch, and G. Pacchioni, Appl. Catal., A **191**, 3 (2000).
[16] J. K. Robert, Proc. R. Soc. London, Ser. A **152**, 445 (1935).
[17] S. Cerny, Surf. Sci. Rep. **26**, 1 (1996).
[18] C. E. Borroni-Bird, N. Al-Sarraf, S. Andersson, and D. A. King, Chem. Phys. Lett. **183**, 516 (1991).
[19] D. A. King, Phys. Scr. **T49**, 506 (1993).
[20] W. A. Brown, R. Kose, and D. A. King, Chem. Rev. **98**, 797 (1998).
[21] R. Kose, W. A. Brown, and D. A. King, Surf. Sci. **402–404**, 856 (1998).
[22] J. T. Stuckless, D. E. Starr, D. J. Bald, and C. T. Campbell, J. Chem. Phys. **107**, 5547 (1997).
[23] J. T. Stuckless, D. E. Starr, D. J. Bald, and C. T. Campbell, Phys. Rev. B **56**, 13 496 (1997).
[24] J. T. Stuckless, N. A. Frei, and C. T. Campbell, Rev. Sci. Instrum. **69**, 2427 (1998).
[25] D. E. Starr, J. T. Ranney, J. E. Musgrove, D. J. Bald, and C. T. Campbell, J. Chem. Phys. **114**, 3752 (2001).
[26] D. E. Starr, D. J. Bald, J. E. Musgrove, J. T. Ranney, and C. T. Campbell (unpublished).
[27] J. T. Ranney, D. E. Starr, J. E. Musgrove, D. J. Bald, and C. T. Campbell, Faraday Discuss. **114**, 195 (1999).
[28] J. H. Larsen, D. E. Starr, and C. T. Campbell, J. Chemical Thermodyn. (to be published).
[29] X. E. Verykios, F. P. Stein, and R. W. Coughlin, Catal. Rev. Sci. Eng. **22**, 197 (1980).
[30] A. Trampert, F. Ernst, C. P. Flynn, H. F. Fischmeister, and M. Rühle, Acta Metall. Mater. **40**, S227 (1992).
[31] U. Schönberger, O. K. Andersen, and M. Methfessel, Acta Metall. Mater. **40**, S1 (1992).
[32] F. Didier and J. Jupille, Surf. Sci. **307–309**, 587 (1994).
[33] M.-H. Schnaffner, F. Patthey, and W.-D. Schneider, Surf. Sci. **417**, 159 (1998).
[34] O. Robach, G. Renaud, and A. Barbier, Phys. Rev. B **60**, 5858 (1999).
[35] G. Renaud, O. Robach, and A. Barbier, Faraday Discuss. **114**, (1999).
[36] A. Barbier, G. Renaud, and J. Jupille, Surf. Sci. **454–456**, 979 (2000).
[37] C. Li, R. Wu, A. J. Freeman, and C. L. Wu, Phys. Rev. B **48**, 8317 (1993).
[38] Y. F. Zhukovskii, M. Alfredsson, K. Hermansson, E. Heifets, and E. A. Kotomin, Nucl. Instrum. Methods Phys. Res. B **141**, 73 (1998).
[39] Y. F. Zhukovskii, E. A. Kotomin, P. W. M. Jacobs, and A. M. Stoneham, Phys. Rev. Lett. **84**, 1256 (2000).
[40] A. V. Matveev, K. M. Neyman, G. Pacchioni, and N. Rösch, Chem. Phys. Lett. **299**, 603 (1999).
[41] A. V. Matveev, K. M. Neyman, I. V. Yudanov, and N. Rösch, Surf. Sci. **426**, 123 (1999).
[42] A. M. Ferrari and G. Pacchioni, J. Chem. Phys. **100**, 9032 (1996).
[43] P. W. Palmberg, T. N. Rhodin, and C. J. Todd, Appl. Phys. Lett. **11**, 33 (1967).
[44] P. Guénard, G. Renaud, and B. Villette, Physica B **221**, 205 (1996).

[45] A. Barbier, Surf. Sci. **406**, 69 (1998).
[46] G. Haas, A. Menck, H. Brune, J. V. Barth, J. A. Venables, and K. Kern, Phys. Rev. B **61**, 11 105 (2000).
[47] D. Chatain, I. Rivollet, and N. Eustathopoulos, J. Chim. Phys.-Chim. Biol. **83**, 561 (1986).
[48] D. Chatain, L. Coudurier, and N. Eustathopoulos, Rev. Phys. Appl. **23**, 1055 (1988).
[49] C. H. F. Peden, K. B. Kidd, and N. D. Shinnm, J. Vac. Sci. Technol. A **9**, 1518 (1991).
[50] K. Hǿjrup Hansen, T. Worren, S. Stempel, E. Lægsgaard, M. Bäumer, H.-J. Freund, F. Besenbacher, and I. Stensgaard, Phys. Rev. Lett. **83**, 4120 (1999).
[51] M.-C. Wu, J. S. Corneille, C. A. Estrada, J.-W. He, and D. W. Goodman, Chem. Phys. Lett. **182**, 472 (1991).
[52] M.-C. Wu, J. S. Corneille, J.-W. He, C. A. Estrada, and D. W. Goodman, J. Vac. Sci. Technol. A **10**, 1467 (1992).
[53] *CRC Handbook of Chemistry and Physics*, edited by D. R. Lide (CRC Press, Boca Raton, FL, 1990).
[54] S. Tanuma, C. J. Powell, and D. R. Penn, Surf. Interface Anal. **17**, 911 (1991).
[55] U. Diebold, J.-M. Pan, and T. E. Madey, Phys. Rev. B **47**, 3868 (1993).
[56] S. C. Parker, A. W. Grant, V. A. Bondzie, and C. T. Campbell, Surf. Sci. **441**, 10 (1999).
[57] J. A. Venables, Philos. Mag. **27**, 697 (1973).
[58] J. A. Venables, Surf. Sci. **299/300**, 798 (1994).
[59] J.-W. He and P. Mǿller, Chem. Phys. Lett. **129**, 13 (1986).
[60] W. R. Tyson and W. A. Miller, Surf. Sci. **62**, 267 (1967).
[61] L. Z. Mezey and J. Giber, Jpn. J. Appl. Phys., Part 1 **21**, 1569 (1982).
[62] M. Methfessel, D. Hennig, and M. Scheffler, Phys. Rev. B **46**, 4816 (1992).
[63] L. Vitos, A. V. Ruban, H. L. Skriver, and J. Kollár, Surf. Sci. **411**, 186 (1998).
[64] J. R. Smith, T. Hong, and D. J. Srolovitz, Phys. Rev. Lett. **72**, 4021 (1994).
[65] R. Sangiorgi, M. L. Muolo, D. Chatain, and N. Eustathopoulos, J. Am. Ceram. Soc. **71**, 742 (1988).
[66] F. Didier and J. Jupille, Surf. Sci. **314**, 378 (1994).
[67] V. Musolino, A. Selloni, and R. Car, J. Chem. Phys. **108**, 5044 (1998).